An integrated photonic-electronic quantum coherent receiver for sub-shot-noise-limited optical links

Volkan Gurses [1,*], Debjit Sarkar [1], Samantha Davis [2], Ali Hajimiri [1]

[1]*Department of Electrical Engineering, California Institute of Technology, Pasadena, CA 91125*
[2]*Department of Physics, California Institute of Technology, Pasadena, CA 91125*

[*]*gurses@caltech.edu*

Abstract: We demonstrate an integrated quantum-limited coherent receiver with co-packaged silicon photonics and electronics. The fully integrated receiver has 2.57 GHz bandwidth, 14.5 dB shot noise clearance, 587 μW knee power, and 2.7×0.8 mm^2 footprint. With this system, we measure squeezed vacuum showing 0.156 ± 0.039 dB sub-shot-noise-level sensitivity.

1. Introduction

Coherent receivers are ubiquitously used in optical networking to form the basis of coherent optical communications. Balanced homodyne detection with quantum-limited coherent receivers also enables measurement of the quadratures of quantum optical states due to their quantum-limited noise floor. Leveraging non-classical states of light in addition to coherent states conventionally used in coherent communications opens up a path to improve the sensitivity of coherent optical links below the shot noise floor and enhance the information capacity of coherent communication systems [1]. Leveraging this sub-shot-noise-level sensitivity with large-scale photonics and electronics has the prospect of impacting many applications in optical communications and sensing.

Silicon photonics offers a promising platform to integrate quantum-limited coherent receivers with high-performance electronics for large-scale quantum optoelectronic circuits, enabling a high level of parallelism in a compact form factor and close interfacing between quantum photonics and electronics. Recently, integrated quantum-limited coherent receivers have been demonstrated to detect non-classical light such as squeezed vacuum [2, 3], and various coherent receivers with quantum-limited sensitivities were demonstrated for quantum communications [4]. In this work, we demonstrate a quantum-limited coherent receiver (QRX) as an electronic-photonic integrated circuit (EPIC) packaged for easy deployment in fiber-optic networks. The QRX has a shot noise clearance (SNC) of 14.5 dB, a knee power (P_{knee}) of 587 μW with 3-dB and shot-noise-limited bandwidths of 2.57 GHz and 3.50 GHz respectively. The packaged EPIC is compact with a total footprint of 2.7×0.8 mm^2.

2. Photonic-Electronic Quantum Coherent Receiver

The photonic integrated circuit (PIC) section of the QRX comprises two edge couplers with 127 μm pitch suitable for coupling the local oscillator (LO) and signal light with fiber arrays, a thermo-optic phase shifter (TOPS) for modulating the phase, a push-pull Mach-Zehnder interferometer (MZI) for interfering LO and signal and correcting the common-mode rejection ratio (CMRR), and a balanced pair of Ge photodiodes (PDs) for photodetection. The electronic integrated circuit (EIC) section of the QRX comprises a transimpedance amplifier (TIA), a voltage amplifier, and an output buffer with differential outputs. As seen in Fig. 1a, The PIC and EIC are packaged together on a custom PCB with a wirebond between the PIC RF output and EIC RF input. To minimize the bond wire parasitics before EIC amplification, pads on both chips were kept level and positioned as close together as possible. RF outputs from the EIC were wirebonded to transmission lines on the PCB matched to 50 Ω. The transmission lines were connected to SMA connectors on the PCB to read out the differential RF outputs. All other DC lines were also wirebonded to the PCB.

The packaged EPIC was first characterized to determine its bandwidth, CMRR, and shot noise clearance to ensure quantum-limited performance. Bandwidth and CMRR measurements were done as a three-port measurement with a 20 GHz vector network analyzer (VNA) connected to the differential outputs of the EIC and a 40 GHz amplitude modulator as seen in Fig. 1a. Current meters were connected to the DC bias lines of the PDs to monitor the PD photocurrents. The optoelectronic response of the QRX is shown in Fig. 1b, showing a 3-dB bandwidth of 2.57 GHz. The CMRR measurement was done by first tuning the MZI on the QRX so that all of the coupled light is illuminated on one PD for the unbalanced frequency response and then tuning the MZI so that both PDs have

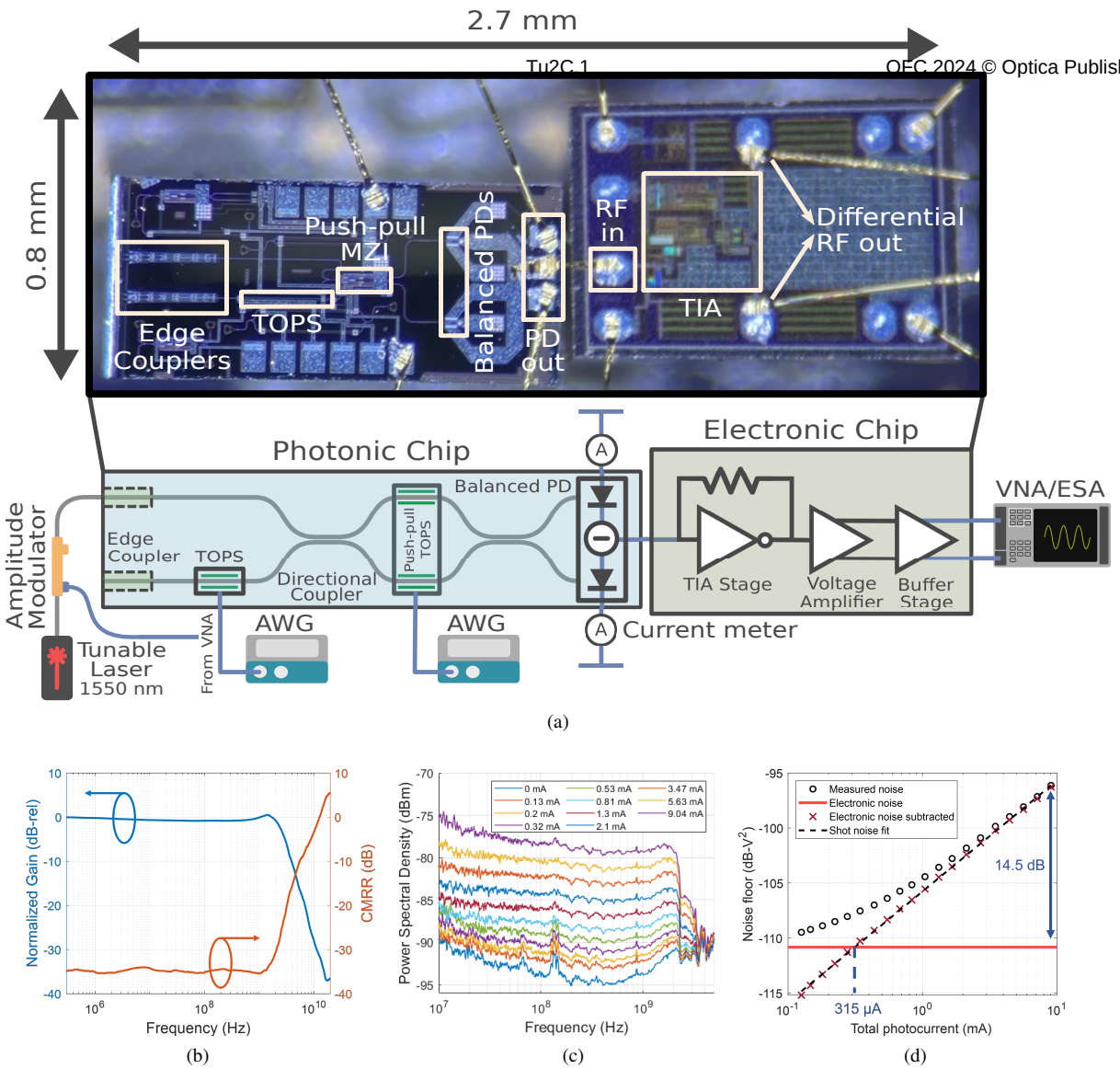

Fig. 1: a) Diagram of the packaged photonic-electronic chip with the characterization setup. b) Measured normalized gain and common-mode rejection ratio response of the QRX. c) Measured noise floor spectra of the QRX at different LO photocurrents. d) Measured total and electronic noise subtracted noise floors integrated over the bandwidth of the QRX with a shot noise fit of slope 1.007 ± 0.015.

the same illumination for the balanced frequency response. Due to the dynamic changes in the coupling coefficients of the on-chip MZI dominated by the drifts in the polarization of the LO over time and the limited dynamic range of the setup, the measurement only gives an upper bound on the CMRR. Gain measurements from the two setups were processed to characterize the CMRR defined as $\text{CMRR} = 10\log_{10}\left(\frac{2P_{bal}}{P_{unb}}\right)$, where P_{bal} and P_{unb} are the balanced RF power and unbalanced RF power measurements, respectively. The resulting CMRR frequency response is seen in Fig. 1b, ensuring a CMRR lower than -35.4 dB.

Shot noise clearance measurements were done with an RF spectrum analyzer (ESA) by sweeping the LO power and measuring the RF spectrum of one of the differential outputs. The photocurrents were monitored to maximize the CMRR and minimize the LO shot noise and relative intensity noise from leaking in [5]. The measurements were also done in a Faraday cage to minimize RF interference from external sources. As seen in Fig. 1c and 1d, the shot noise clearance is 14.5 dB over the bandwidth of the QRX. The SNC frequency response with maximum LO photocurrent is seen in Fig. 2c, showing a shot-noise-limited bandwidth of 3.50 GHz. A shot noise line is also fitted to the electronic noise subtracted measurements showing a near-unity slope of 1.007 ± 0.015, ensuring broadband quantum-limited performance.

3. Squeezed Light Measurements

The QRX was used to measure squeezed vacuum to demonstrate sub-shot-noise level operation up to the shot-noise-limited bandwidth. The squeezed vacuum was generated with two periodically-poled lithium niobate (PPLN) waveguides cascaded with reverse polarities for SHG and SPDC as seen in Fig. 2a. Squeezed vacuum

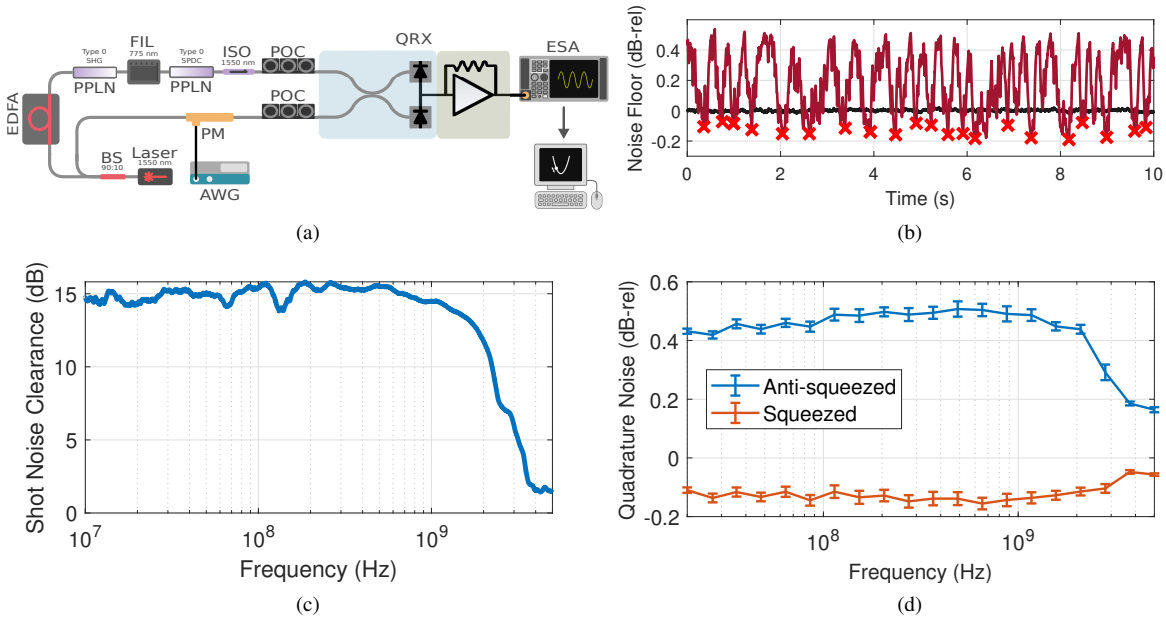

Fig. 2: a) Setup with the integrated photonic-electronic coherent receiver for squeezed light measurements. b) Oscillations between quadratures of the squeezed vacuum measured at 1.17 GHz. Red crosses signify the squeezed quadrature. c) Shot noise clearance response of the QRX with maximum LO photocurrent. d) Quadrature noise normalized to the shot noise level of vacuum for squeezed and anti-squeezed quadratures.

was coupled to chip with a V-groove array. Noise floor oscillations in the output with 1 Hz LO phase modulation were measured with a spectrum analyzer at different sideband frequencies. 30-second traces were recorded for both squeezed vacuum (red) and vacuum (black) at each frequency. A 10-second section of the data measured at 1.17 GHz is shown in Fig. 2b. After data collection, a peak search algorithm was used to acquire the noise level for squeezed and anti-squeezed quadratures normalized to the shot noise level (SNL) at each frequency as shown in Fig. 2d. A maximum squeezed noise of 0.156 ± 0.039 dB below the SNL and a maximum anti-squeezed noise of 0.507 ± 0.052 above the SNL were observed.

While we were limited by the source and tabletop component losses in the squeezed light measurements, on-chip loss sets the bound on how much squeezing can be observed with the QRX. The on-chip system loss comprises the optical losses and the optoelectronic loss determined by the shot noise clearance and PD quantum efficiency (QE). The QRX has a total optical loss of 2.7 dB with 1.3 dB from edge couplers, 1.4 dB from PD QE, and a negligible amount of loss from the TOPS, MZI, and routing. As shown in Fig. 2c, the shot noise clearance is also greater than 10 dB up to 2.24 GHz. Therefore, the system loss is at most 3 dB over the bandwidth of the receiver, enabling sensitivities of 3 dB below the SNL.

4. Conclusion

The packaged photonic-electronic QRX enables a path toward the deployment of quantum-limited coherent receivers in optical communication and sensing networks. Due to its compact size, high CMRR, highest reported 3-dB bandwidth and lowest reported system loss in the literature, it introduces the prospect of leveraging non-classical states of light to enhance the information capacity and sensitivity of optical links. With the demonstration of high shot-noise-limited bandwidth and detection of squeezed vacuum showcasing an enhancement in the SNL, this work highlights the potential of leveraging non-classical light and deploying quantum coherent receivers in classical optical networks in addition to preparing an infrastructure suitable for quantum communications.

References

1. K. Banaszek, L. Kunz, M. Jachura, and M. Jarzyna, "Quantum limits in optical communications," J. Light. Technol. **38**, 2741–2754 (2020).
2. V. Gurses, S. I. Davis, E. Knabe, R. Valivarthi, M. Spiropulu, and A. Hajimiri, "A compact silicon photonic quantum coherent receiver with deterministic phase control," in *2023 Conference on Lasers and Electro-Optics,* (2023), pp. 1–2.
3. J. F. Tasker *et al.*, "Silicon photonics interfaced with integrated electronics for 9 ghz measurement of squeezed light," Nat. Photonics **15**, 11–15 (2021).
4. C. Bruynsteen, M. Vanhoecke, J. Bauwelinck, and X. Yin, "Integrated balanced homodyne photonic–electronic detector for beyond 20ghz shot-noise-limited measurements," Optica **8**, 1146–1152 (2021).
5. B. V. Gurses and A. Hajimiri, "Performance limits of sub-shot-noise-limited balanced detectors," in *Frontiers in Optics + Laser Science 2022,* (Optica Publishing Group, 2022), p. JW4A.32.